

RESEARCH

Open Access



Characterization of tumor prognosis and sensitive chemotherapy drugs based on cuproptosis-related gene signature in ovarian cancer

Wei Tan^{1†}, Fangfang Dai^{1†}, Qinyu Ci¹, Zhimin Deng¹, Hua Liu^{1*} and Yanxiang Cheng^{1*}

Abstract

Background Cuproptosis is a novel form of cell death, acting on the tricarboxylic acid cycle in mitochondrial respiration and mediated by protein lipoylation. Other cancer cell death processes, such as necroptosis, pyroptosis, and ferroptosis, have been shown to play crucial roles in the therapy and prognosis of ovarian cancer. However, the role of cuproptosis in ovarian cancer remains unclear.

Methods The expression profiles of 10 cuproptosis-related genes were extracted from GSE140082. Kaplan-Meier survival and Cox proportional hazards regression were used to identify prognostic genes for constructing risk models. Following this, Least Absolute Shrinkage and Selection Operator regression was employed to construct a risk score model. Next, a nomogram was constructed to predict overall survival in ovarian cancer. Ultimately, our analysis compared the two groups across various dimensions, including clinical characteristics, tumor progression, metabolism-related pathways, immune landscape, and drug sensitivity.

Results MTF1 and LIAS were identified as protective factors in ovarian cancer, with patients in the higher risk group being significantly associated with poorer survival. Furthermore, integrating the risk score with clinical characteristics in the nomogram demonstrated high specificity and sensitivity in predicting survival. A higher proportion of M2 macrophages, follicular helper T cells, and resting mast cells was observed in the high-risk group. Additionally, the IC50 values of Dasatinib, Bortezomib, Parthenolide, and Imatinib were significantly lower in the high-risk group.

Conclusions The study highlights the prognostic significance of cuproptosis-related genes and provides new insights into developing pharmacological therapeutic strategies targeting cuproptosis for the prevention and treatment of ovarian cancer.

Keywords Cuproptosis, Ovarian cancer, Prognosis, Chemotherapy, Immunotherapy

[†]Wei Tan and Fangfang Dai contributed equally to this work.

*Correspondence:

Hua Liu

liuhua008@tom.com

Yanxiang Cheng

yanxiangCheng@whu.edu.cn

¹ Department of Obstetrics and Gynecology, Renmin Hospital of Wuhan University, Wuhan 430060, China

Background

Ovarian cancer is one of the most lethal gynecologic malignancies worldwide, with high mortality rates [1]. According to the latest information in national cancer institute, the death rate of ovarian cancer was 6.3 per 100,000 women per year, and the 5-year relative survival was 49.7%. Due to challenges in early diagnosis, over 70% of patients are diagnosed at stages III-IV, which



significantly impacts the prognosis of women with ovarian cancer [2]. Currently, the treatment of ovarian cancer relies on debulking surgery and chemotherapy. Additionally, inhibitors targeting poly ADP-ribose polymerase have been incorporated as first-line therapy for women with BRCA1/BRCA2 mutations [3]. However, many patients still lack viable late-stage therapeutic options and effective treatments. There is an urgent need to identify predictive biomarkers that can improve patient outcomes with chemotherapy, molecular targeted therapy, or immunotherapy.

A novel mechanism of cell death induced by copper was identified and termed “cuproptosis” by Tsvetkov and colleagues in the journal ‘Science’. This mechanism is distinct from other known cell death processes such as apoptosis, pyroptosis, anoikis, and ferroptosis [4]. Excess copper within cells can be transported to the mitochondria by ionophores. The increased copper directly binds to lipoylated components of the tricarboxylic acid (TCA) cycle, leading to proteotoxic stress and eventual cell death [4]. In various malignant tumors, including breast cancer, lung cancer, and prostate cancer, significant alterations in the accumulation levels of Cu in serum and tumor tissues have been observed [5–7]. Copper, an essential trace element, can influence tumorigenesis, angiogenesis, tumor recurrence, metastasis, and drug resistance by binding to and activating key molecules in multiple signaling pathways [8, 9]. The discovery of cuproptosis reveals interaction patterns between transition metals and proteins, highlighting the intricate connections between copper and tumor progression. This insight provides a new strategy for achieving precise diagnosis and treatment of malignant tumors. Lu et al. designed a nano-material loaded with epirubicin (copper ionophore) and copper, which significantly inhibits the growth of melanoma [10]. Furthermore, Guo and his colleagues designed a reactive oxygen species-sensitive polymer for co-encapsulation of epirubicin and copper, forming nano-particles (NP@ESCu). They discovered that NP@ESCu not only promotes cancer cell death but also binds to PDL1, enhancing the immune response to achieve anti-cancer effects [11]. Therefore, enhancing the understanding of cuproptosis in tumor cells enables us to wield this sword against cancers effectively.

In ovarian cancer, Lin and Yang identified increased circulating copper levels in ovarian cancer patients [12]. Moreover, several studies have indicated that copper is associated with platinum drug resistance in ovarian cancer, highlighting its potential for developing novel cancer therapies [13–15]. Other cell death processes like necroptosis, pyroptosis, and ferroptosis have been shown to play crucial roles in therapy and prognosis in ovarian

cancer [16–18]. However, the specific role of cuproptosis in ovarian cancer remains unclear.

In this study, we analyzed the expression of ten cuproptosis-related genes in ovarian cancer and explored the frequency of Copy Number Variation (CNV) in these genes. Information on these ten cuproptosis-related genes has been previously documented elsewhere, detailing their specific functions and roles in cuproptosis (see Additional file 1) [19]. Subsequently, survival analysis revealed that Metal Regulatory Transcription Factor 1 (MTF1) and Lipoic Acid Synthetase (LIAS) act as protective factors for ovarian cancer patients. Furthermore, a prognostic model was established using univariate Cox analysis and least absolute shrinkage and selection operator (LASSO) regression analysis. We also examined the clinical characteristics, tumor progression, metabolism-related pathways, immune landscape, and drug sensitivity in two risk groups of ovarian cancer patients, revealing significant distinctions between the groups. The evaluation of our risk model showed promising potential for guiding therapy in ovarian cancer. These findings elucidate the molecular mechanisms involving LIAS and MTF1, suggesting they could serve as potential therapeutic targets for ovarian cancer.

Methods

Data collection and preprocessing

The expression profiles and clinical information of ovarian cancer were obtained from The Cancer Genome Atlas (TCGA, <https://portal.gdc.cancer.gov/>) and the expression matrix of normal ovarian tissue was acquired from the Genotype-Tissue Expression (GTEx, <http://commonfund.nih.gov/GTEx/data>). GTEx collects and provides normal samples from various organs and tissues, which can be used to analyze transcriptomic characteristics of tissues under disease conditions, helping us understand and compare gene expression changes associated with diseases [20]. GSE140082 and GSE63885 from the Gene Expression Omnibus (GEO, <https://www.ncbi.nlm.nih.gov/geo/>) database were downloaded. Furthermore, the expression data of 10 cuproptosis-related genes (CDKN2A, FDX1, DLD, DLAT, LIAS, GLS, LIPT1, MTF1, PDHA1 and PDHB) were extracted. Expression differences between ovarian cancer and normal samples were calculated using the “limma” package (Australia, 2015, version:3.52.4) within the R (version: 4.4.1) software environment for statistical computing. Significance analyses were conducted using unpaired Wilcoxon rank sum and signed rank tests. The Sangerbox database (<http://www.sangerbox.com/>) was used for visualization. Correlation analysis of ten cuproptosis-related genes were estimated with a Spearman analysis using the R package “psych” (American, 2024, version: 2.4.6.26). The

“corrplot” package (American, 2021, version: 0.92) was applied for visualization.

Copy number variation

The CNV was obtained from TCGA dataset. Gene Set Cancer Analysis (<http://bioinfo.life.hust.edu.cn/GSCA/#/>) was applied for exploring the correlations of CNV with mRNA expression in ovarian cancer.

Survival analysis

For Kaplan–Meier (KM) curves, p values and hazard ratio (HR) with 95% confidence interval (CI) were generated using log-rank tests using R packages “ggrisk” (China, 2021, version: 1.3), “survival” (2024, version:3.6–4), “survminer” (2021, version: 0.4.9), and “timeROC” (2019, version: 0.4) were applied in the process. $p < 0.05$ was considered statistically significant. Additionally, the online database Kaplan–Meier Plotter (<https://kmpplot.com/analysis/>) which integrates data from GEO, the European Genome-phenome Archive (<https://www.ebi.ac.uk/ega/>) and TCGA was employed to validate the relationship between LIAS or MTF1 and the overall survival (OS) of ovarian cancer patients [21].

Construction of the risk score model

Univariate Cox regression analysis was applied to screen prognostic cuproptosis-related genes using R “Survival” package (2024, version:3.6–4). Next, the LASSO regression was employed to construct risk score model using R package “glmnet” (2023, version:4.1–8).

The R “Survminer” package (2021, version: 0.4.9) was utilized to determine cutoff points, and the patients were then divided into the high- and low-risk group based on cutoff points. Patients with risk scores above the cutoff were assigned to the high-risk group. Conversely, patients with risk scores below the cutoff were assigned to the low-risk group.

Establishment of a prognostic nomogram

When constructing the multivariate Cox regression, we obtained the regression coefficient β (coef) for each variable. The nomogram prediction model is essentially a visualization of the multivariate Cox regression. The Nomogram normalizes the regression coefficients and displays them as risk scores on a number line, mapping the predicted probability to a scale from 0 to 100. The total score accumulated from the various covariates corresponds to the patients’ predicted probability, representing the relative importance of each variable in the model. The subvariables of individual covariates were quantified as scores, and the corresponding probability of the total score after adding each subvariable possessed by the patient was used as the predicted result. The nomogram

was established according to the method previously reported [22]. Receiver operating characteristic (ROC) (R package “survivalROC”, 2022, version: 0.4.9) curves were constructed to evaluate the prognostic ability of the nomogram for 1/2/3-year OS and to calculate the area under the curve (AUC) values.

Functional analysis

The Search Tool for the Retrieval of Interacting Genes (<https://cn.string-db.org/>) protein database was utilized to construct the Protein-protein interactions (PPI) and co-expression networks [23]. Next, Gene Ontology (GO) and Kyoto Encyclopedia of Genes and Genomes (KEGG) enrichment analyses were performed based on the ten cuproptosis-related genes using the R packages “clusterProfiler” (China, 2021, version: 4.0). The significance criteria were set at $p < 0.05$. Four tumor-related biology pathways (angiogenesis, epithelial-mesenchymal transition (EMT), glycolysis, and hypoxia) were downloaded from the molecular signature database (<https://www.gsea-msigdb.org/gsea/msigdb/index.jsp>). Furthermore, we acquired four metabolic signature gene sets previously reported, including amino acid metabolism, carbohydrate metabolism, lipid metabolism and tricarboxylic acid cycle [24]. Gene Set Variation Analysis (GSVA) is a method used to assess the relative activity levels of gene sets within individual samples, particularly useful for analyzing scores related to tumor progression and metabolism-related pathways. For each sample, the R-package “GSVA” (Spanish, 2022, version: 1.44.5) was used to calculate the relative activity level for each selected gene set. GSVA transforms gene expression values within each gene set into a single sample-specific score, enabling comparison of gene set activity levels across different samples. Analysis of GSVA scores identifies pathways potentially crucial in tumor progression. Higher GSVA scores typically indicate active pathways associated with tumor progression within the sample, whereas lower scores suggest lower activity in those pathways.

Immune cell infiltration

In order to evaluate the correlation between risk group and immune cell infiltration in ovarian cancer, the proportions of tumor-infiltrating immune cells were calculated using ‘CIBERSORT’, containing the expression features of 22 immune cell subtypes (<https://cibersortx.stanford.edu/>) [25]. Furthermore, single-cell analysis of LIAS and MTF1 in ovarian cancer was conducted in the Tumor Immune Single-Cell Hub (TISCH, <http://tisch.comp-genomics.org/>) database [26]. Tumor Immune Dysfunction and Exclusion (TIDE, <http://tide.dfci.harvard.edu/>) platform was used to evaluate the effectiveness of immunotherapy between two risk groups [27].

Drug sensitivity

The Cellminer database (<https://discover.nci.nih.gov/cellminer/home.do>) was established by the National Cancer Institute [28]. Food and Drug Administration (FDA) approved, clinically tested drugs were selected. Next, correlation analysis was performed between the RNA expression level of LIAS and MTF1 and the drug sensitivity. Finally, boxplots were generated to illustrate the differences in platinum sensitivity between two groups, divided based on high or low expression levels of LIAS and MTF1.

We collected the data of drug sensitivity and the mRNA expression of LIAS and MTF1 from the Cancer Therapeutics Response Portal (CTRP, <https://portals.broadinstitute.org/ctrp/>) and Genomics of Drug Sensitivity in Cancer (GDSC, <https://www.cancerrxgene.org/>) databases. Spearman correlation analysis was performed to assess the relationship between gene mRNA expression and the drug IC50 values. A bubble plot was used to summarize the correlations between LIAS or MTF1 and drugs sensitivity.

Statistical analysis

The R software (version 4.4.1) was employed to perform the analysis. R package “ggplot2” (American, 2024, version: 3.5.1) was used for visualization. For comparisons between two groups, if the samples meet the parameter conditions (normal distribution and homogeneity of variance), t test was employed, otherwise the non-parametric two-sided Wilcoxon-rank sum test was performed. $p < 0.05$ was considered statistically significant.

Results

The expression of cuproptosis-related genes in ovarian cancer

Firstly, we explored the differential expression of ten cuproptosis-related genes in ovarian cancer. The results suggested that the expression of four cuproptosis-related genes (CDKN2A, FDX1, DLAT and PDHB) were elevated in ovarian cancer, while the expression of LIAS, MTF1, GLS, LIPT1 and PDHA1 were decreased (Fig. 1A). In addition, there were strong associations between the expression of ten cuproptosis-related genes (Fig. 1B). For instance, FDX1 was highly and positively correlated with DLAT ($r = 0.79$, $p < 0.001$) (Fig. 1B). Next, we explored the CNV frequency of the cuproptosis-related genes, and revealed that a larger number of broad CNVs were existed in these genes, most of which led to amplification, except for deletions in FDX1, DLAT, PDHB and PDHA1 (Fig. 1C). Furthermore, CNV was shown to be positively correlated with the expression of cuproptosis-related genes (Fig. 1D).

The prognostic value of cuproptosis-related genes and construction of the risk model

GSE140082, which includes the expression profiles and clinical information of 380 ovarian cancer patients, was used to study the prognosis of 10 cuproptosis-related genes. We observed that MTF1 and LIAS act as protective factors for ovarian cancer patients (Fig. 2A and B). Using the KMplotter website to validate the prognostic effects of LIAS and MTF1, the results indicated that high expression of LIAS and MTF1 was associated with a favorable prognosis (Additional file 2). Furthermore, univariate Cox analysis revealed that MTF1 and LIAS were protective factors for ovarian cancer, consistent with the survival analysis (Fig. 2C). Subsequently, MTF1 and LIAS were selected to construct a prognostic model using LASSO regression analysis. Based on the optimal cutoff value, patients were categorized into high or low-risk groups (Fig. 2D). Survival analysis showed that a higher risk score was significantly associated with poorer overall survival (OS) (Fig. 2E). Moreover, the predictive performance of the risk model was deemed satisfactory (Fig. 2F).

Construction and validation of a prognostic nomogram

We examined the prognostic effects of the risk model in patients at different clinical stages. Patients with high-risk scores, in terms of age, grade 3–4, and stage III-IV had significantly worse overall survival (OS) compared to those with low-risk scores (Additional file 3A-D). However, due to the challenges in early detection of ovarian cancer, most clinical samples were found to be in intermediate to advanced stages, resulting in a small number of patients with G1-2 and stage I-II, which may bias the experimental results (Additional file 3E and 3F). The risk score was identified as an independent protective factor ($p < 0.001$, 95% CI HR: 1.215–1.516) (Fig. 3A), and this association remained statistically significant ($p < 0.001$, 95% CI HR: 1.195–1.486) after adjusting for age, stage, and grade (Fig. 3B). To provide a quantitative method for survival prediction, we constructed a nomogram integrating both the risk score and clinical characteristics (Fig. 3C). The overall C-index of the model was 0.69. Calibration plots depicted in Fig. 3D demonstrated good performance of the derived nomogram. Similarly, the nomogram model showed predictive ability for 1, 2, and 3-year overall survival rates (1-year AUC = 0.67, 2-year AUC = 0.73, 3-year AUC = 0.68) (Fig. 3E), indicating high specificity and sensitivity in survival prediction when integrating the risk score with clinical characteristics. Additionally, external datasets GSE63885 and TCGA were used for validation to assess the prognostic value of the risk scores. The results confirmed that high-risk

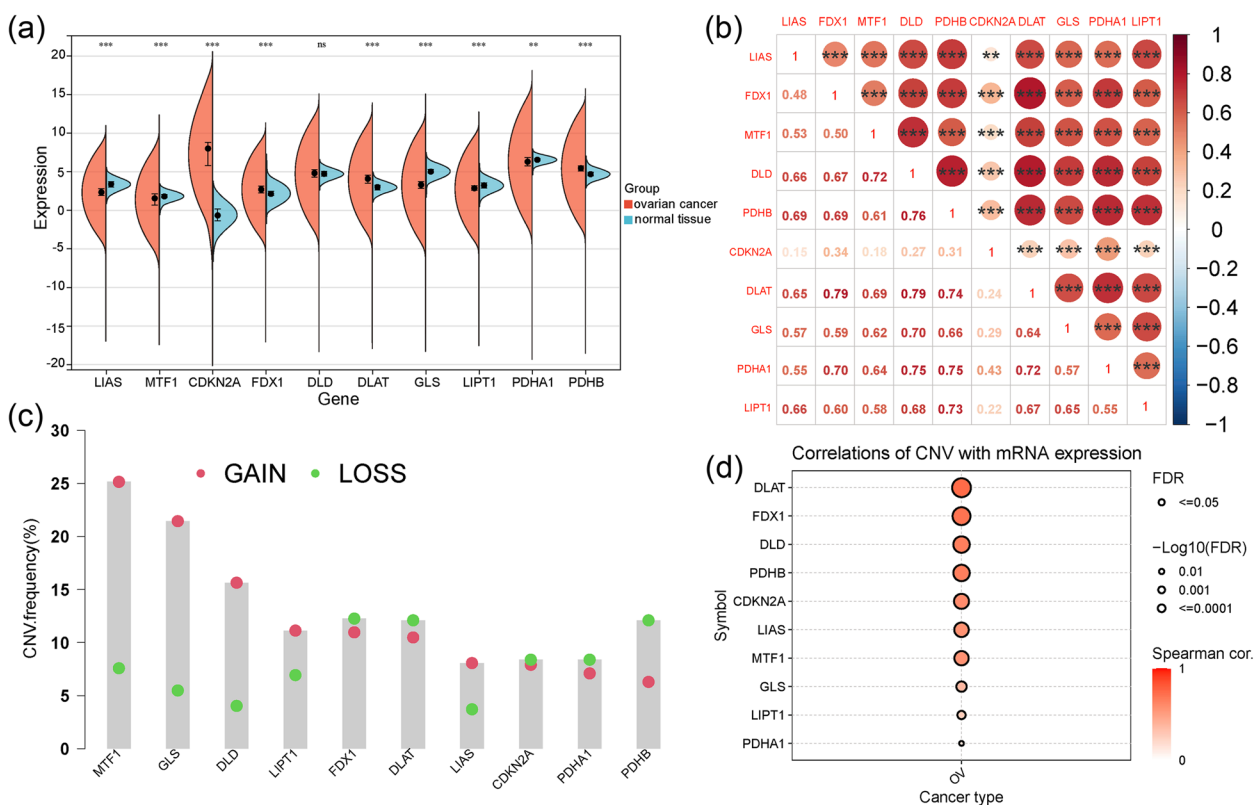


Fig. 1 The expression and CNV landscape of cuproptosis-related genes in ovarian cancer. **A** Significant differences in the mRNA levels of cuproptosis-related genes in ovarian cancer versus normal tissues. Red represents ovarian cancer whereas blue represents normal ovarian tissue. **B** Correlation analysis of cuproptosis-related genes in ovarian cancer. Red represents a positive correlation while blue represents a negative correlation. The values in the bottom triangle represents the correlation coefficients. **C** Frequencies of CNV gain and loss CNV among cuproptosis-related genes. **D** Spearman correlation between CNV and mRNA expression of cuproptosis-related genes in ovarian cancer. The larger the circle, the smaller log-rank value. The redder the color, the stronger the correlation. *** $p < 0.001$, ** $p < 0.01$. ns means no statistical difference

scores were strongly associated with worse prognosis (Fig. 3F).

Functional analysis

The PPI analysis revealed that PDHB, LIAS, DLAT, PDHA1, LIPT1, and DLD exhibited numerous internal connections with other proteins, whereas CDKN2A and MTF1 were not associated with others (Fig. 4A). To further elucidate the potential roles of cuproptosis-related genes, functional enrichment analyses, including GO and KEGG pathway analyses, were conducted.

The GO analysis results showed that cuproptosis-related genes were associated processes such as mRNA metabolic processes, mRNA stability, ubiquitin ligase complex, methyltransferase complex, ubiquitin-protein transferase activity, and methylation-dependent protein binding (Fig. 4B). Furthermore, KEGG pathway analysis revealed involvement in pathways including ubiquitin-mediated proteolysis, mitophagy, RNA polymerase,

adherens junction, and Hedgehog signaling pathways (Additional file 4).

Additionally, we investigated the relationship between risk groups and pathways related to tumor progression and metabolism. In GSE140082, angiogenesis and EMT were enriched in the high-risk group, whereas amino acid metabolism was enriched in the low-risk group (Fig. 4C). Consistent results were observed in GSE63885 and TCGA datasets (Fig. 4D and E).

Immune landscape

The infiltration level of immune cells was evaluated in the GSE140082 cohort using the CIBERSORT algorithm (Fig. 5A). Patients in the two groups showed no difference in the infiltration of most antitumoral immune cells, including CD8⁺ T cells, activated NK cells, memory CD4⁺ T cells, and activated dendritic cells. However, the high-risk group exhibited a higher fraction of CD4⁺ native T cells ($p < 0.01$), M2 macrophages ($p < 0.001$), follicular helper T cells ($p < 0.05$), and resting

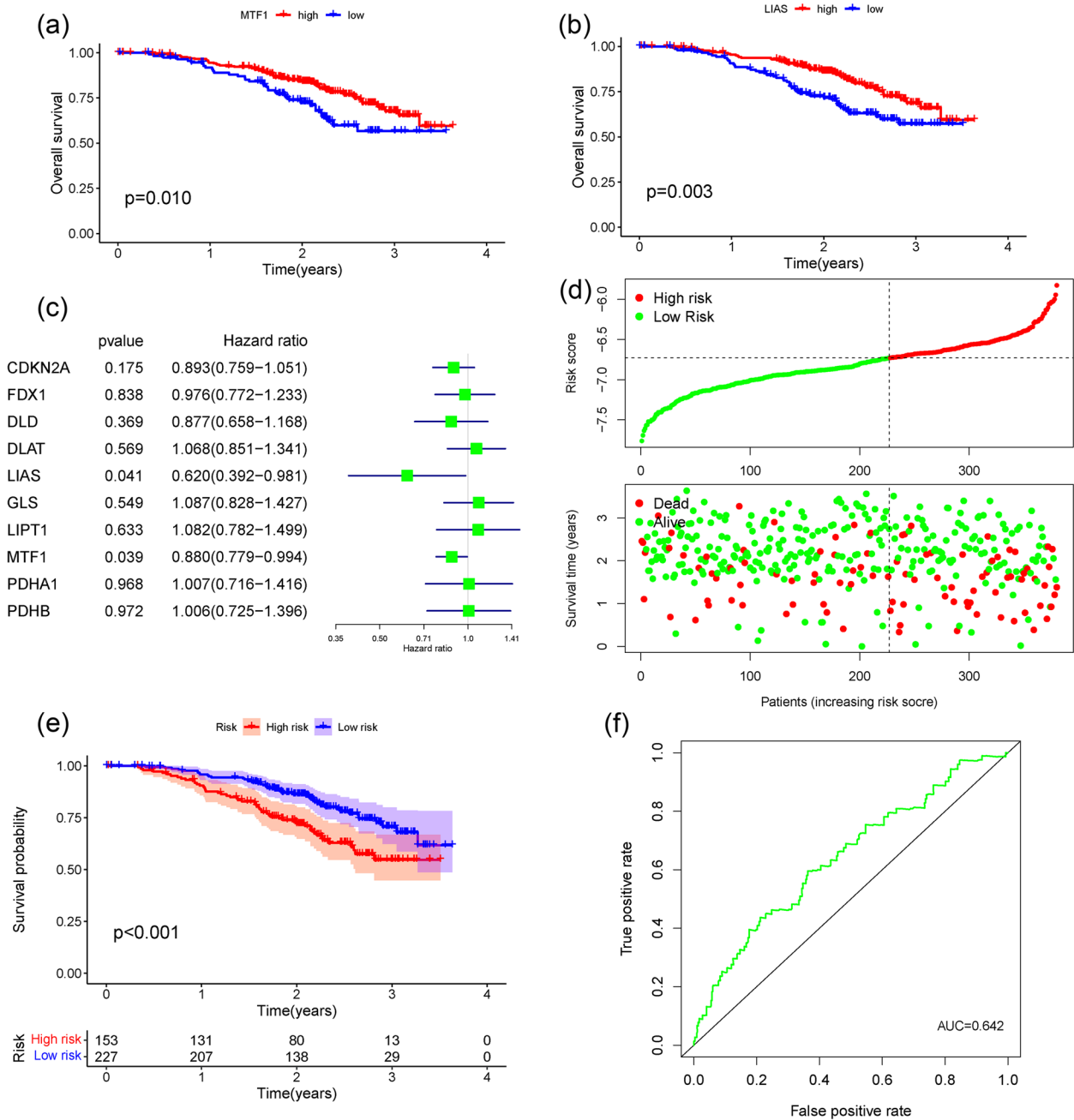


Fig. 2 The prognostic value of cuproptosis-related genes and construction of the risk model. High expression of MTF1 (A) and LIAS (B) were associated with better overall survival. C Univariate analysis of the hazard ratios for cuproptosis-related genes. D The risk score and survival time in GSE140082. E Survival analyses for patients in high- and low- risk group using Kaplan-Meier curves. F Receiver operating characteristic (ROC) curves of risk model

mast cells ($p < 0.05$). Additionally, a higher level of monocytes ($p < 0.01$) was observed in ovarian cancer patients from the low-risk group (Fig. 5A).

Next, we explored the association between the expression of LIAS or MTF1 and immune cells. We obtained single-cell RNA sequencing data of ovarian cancer

samples in GSE147082 cohort using the TISCH2 website (Additional file 5 A and 5B). The results indicated that LIAS and MTF1 were detectable in both tumor cells and non-tumor cells (Additional file 5C and 5D). LIAS expression was predominantly detected in T cells, B cells, and macrophages (Additional file 5E), while both LIAS

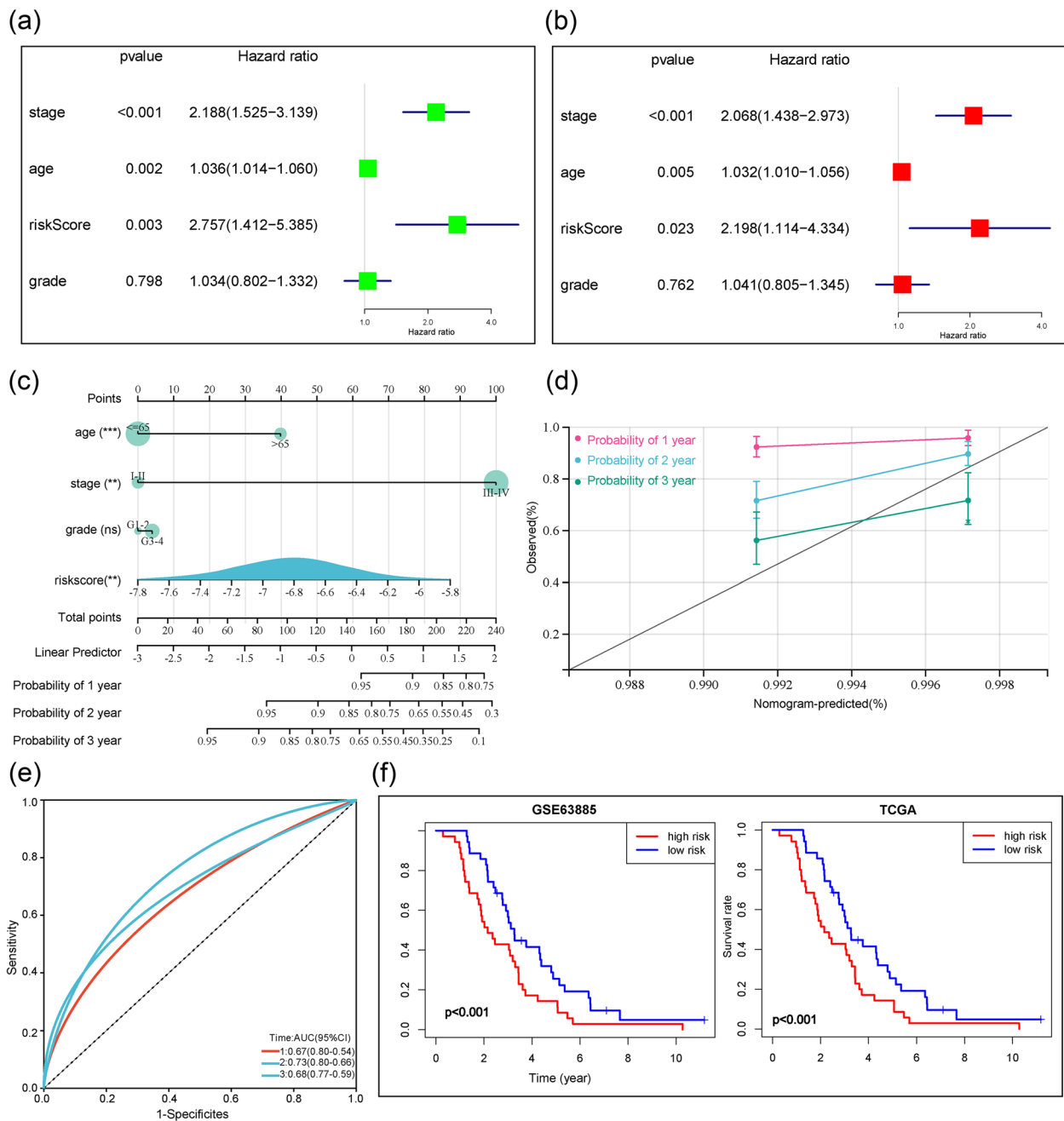


Fig. 3 Validation and application of risk score in ovarian cancer. **A, B** Univariate analysis (**A**) and multivariate analysis (**B**) of the hazard ratios for the risk score. **C** A nomogram to quantitatively predict survival based on the risk score and clinical parameters. **D** Calibration curves of the nomogram and receiver operating characteristic (ROC) curves (**E**) to estimate the accuracy and performance of the predictive nomogram. **F** Validation of risk score in GSE63885 and TCGA. *** $p < 0.001$, ** $p < 0.01$. ns means no statistical difference

and MTF1 were enriched in B cells, macrophages, and endothelial cells (Additional file 5F).

Furthermore, using TIMER datasets, we analyzed the correlation between LIAS or MTF1 expression and immune cells infiltration. The results revealed that LIAS was positively correlated with CD4 and CD8+ T cells,

and MTF1 was positively correlated with macrophages, which corroborated with the single-cell RNA sequencing results (Additional file 6A). Considering the clinical use of immune checkpoint inhibitors (ICIs) in ovarian cancer treatment, we investigated the association between risk score and the expression levels of ICI-related biomarkers.

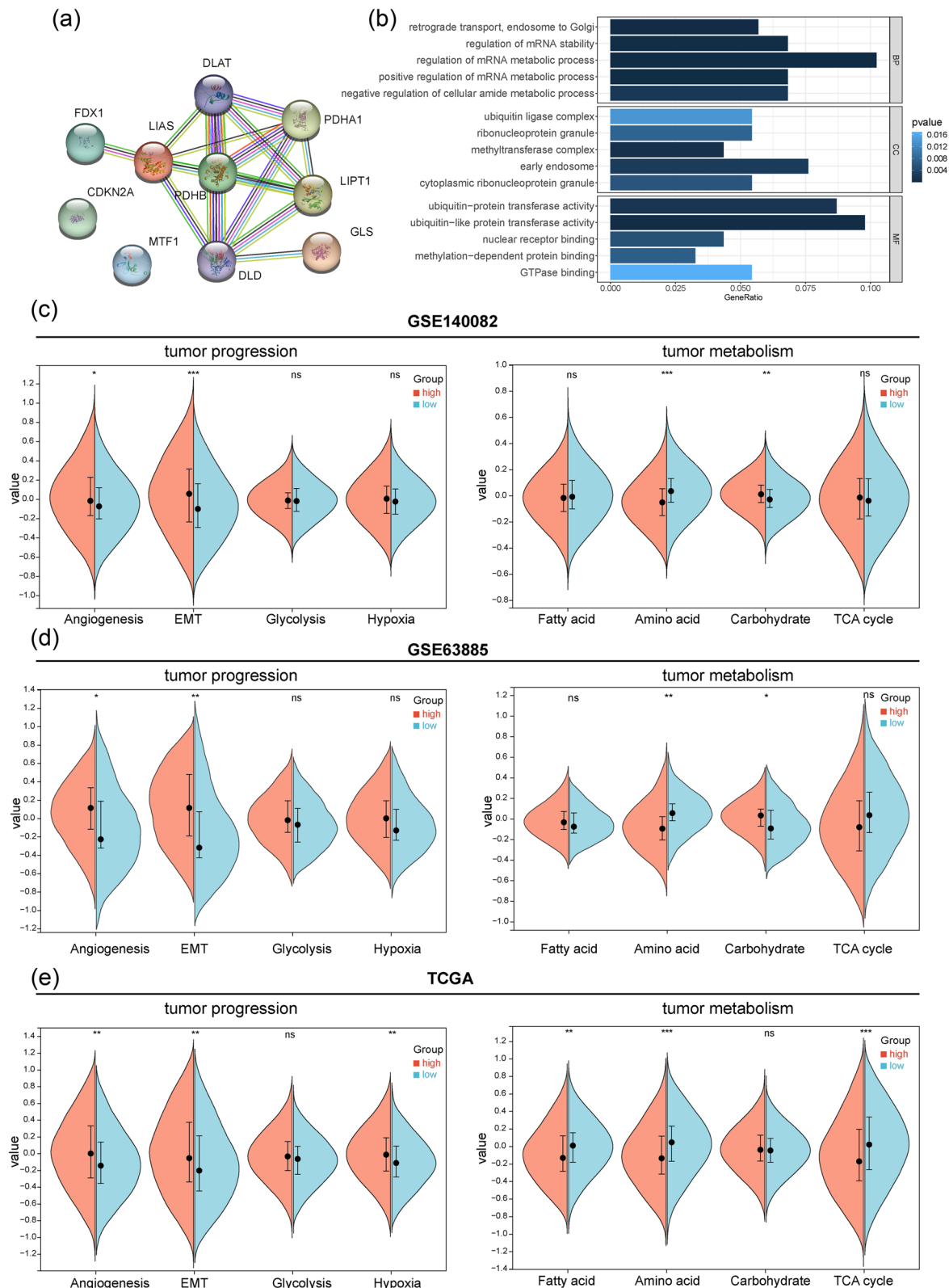


Fig. 4 The functional analysis of cuproptosis-related genes. **A** The PPI network of ten cuproptosis-related genes. **B** The GO analysis of cuproptosis-related genes. **C-E** The enrichment score of tumor progression and tumor metabolism between two risk groups in GSE140082 (**C**), GSE63885 (**D**) and TCGA (**E**). *** $p < 0.001$, ** $p < 0.01$, * $p < 0.05$. ns means no statistical difference

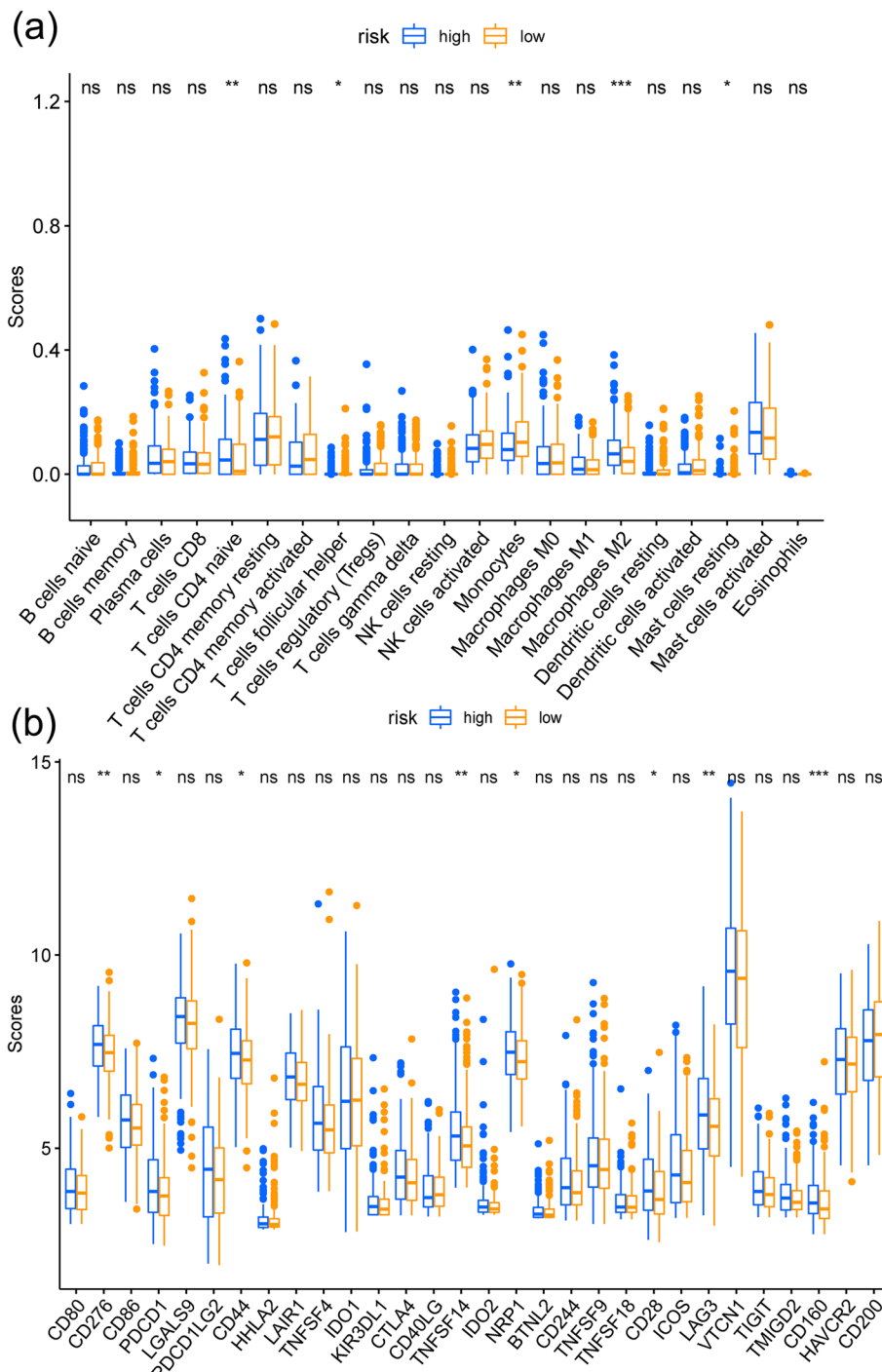


Fig. 5 The immune landscape in risk groups. **A** and **B** The abundance of tumor immune infiltrating cell (**A**) and the expression of immune checkpoint (**B**) between two risk groups

We found that high risk scores were positively correlated with elevated expression of CD276, PDCD1, CD44, LAG3, and CD160 (Fig. 4B). The TGF-β pathway plays a critical role in the immunosuppressive tumor

microenvironment, and we observed up-regulation of TGF-β-related genes in the high-risk group (Additional file 5B). These findings suggest that the immune microenvironment in the high-risk group is more prone to an

immunosuppressive state. Additionally, the high-risk group exhibited a higher TIDE score, indicating a greater potential for immune escape (Additional file 5 C).

Drug sensitivity analysis

Drug sensitivity analysis was conducted to identify potentially responsive drugs. Results with $p < 0.05$ and $\text{cor} > 0.3$ were exclusively included in additional file 6. Positive correlations were observed between the IC50 values of 15 drugs (Palbociclib, Nelarabine, Chelerythrine, Fostamatinib, Vorinostat, Hydroxyurea, Asparaginase, Dromostanolone Propionate, Cytarabine, Acrichine, Cladribine, Nitrogen mustard, Cyclophosphamide, LMP776, and Crizotinib) and LIAS levels in ovarian cancer patients. Conversely, negative correlations were found between the By-Product of CUDC-305 and MTF1. Subsequently, we investigated differences in drug reactivity IC50 values between high- and low-LIAS groups. Specifically, the IC50 values of six drugs (Palbociclib, LMP776, Vorinostat, Dromostanolone Propionate, Nitrogen mustard, and Cladribine) were lower in the low-LIAS group (Additional file 8 A-F). These findings suggest a potential efficacy of these six drugs in treating LIAS-related conditions. Genomic alterations have a considerable impact on the clinical response to chemotherapy. We further integrated drug sensitivity data with gene expression profiles from GDSC and CTRP cancer cell lines databases. In the CTRP database, drug sensitivity to gemcitabine, vincristine, SR-II-138 A, CR-1-31B, and KX2-391 showed a negative correlation with MTF1 or LIAS expression levels (Additional file 9 A). Pearson's correlation analysis in the GDSC database revealed that drug sensitivity to AT-7519, PHA-793,887, and SNK-2112 was negatively associated with MTF1 and LIAS levels based on IC50 values (Additional file 9B).

The above studies primarily focused on the expression levels and drug sensitivity of LIAS and MTF1. To explore drug sensitivity in the high- and low-risk groups, we employed ridge regression analysis using the pRRophetic algorithm to estimate the IC50 of drugs in each ovarian cancer patient. We observed that the IC50 values of Dasatinib, Bortezomib, Parthenolide, and Imatinib were significantly lower in the high-risk group ($p < 0.05$; Fig. 6A-D), suggesting that patients in the high-risk group tended to be more sensitive to chemotherapy.

Discussion

Ovarian cancer presents significant challenges in treatment and prognosis due to its difficulty in early detection, high malignancy, propensity for distant metastasis, and tendency for recurrence. Besides surgical intervention, ovarian cancer typically requires adjunctive therapies to prevent relapse. Chemotherapy stands as the mainstay

of treatment, yet some patients develop resistance to chemotherapy drugs. Additionally, targeted therapies directed at specific biomarkers and genetic mutations in cancer cells, such as PARP inhibitors, BRAF inhibitors, and mitogen-activated protein kinase kinase (MEK) inhibitors, offer personalized treatment options [29, 30]. However, there remains a lack of universally applicable targeted therapies for all ovarian cancer patients, as some tumors may not harbor identifiable biomarkers or mutations suitable for targeted treatments. Therefore, there is an urgent need for exploring new potential therapeutic avenues to improving the prognosis and survival rates of ovarian cancer patients.

Extensive evidence suggests that copper levels are elevated in various malignant tumors [31–33]. Intracellular copper release is facilitated by GSH redox activity. When copper accumulates excessively in cancer cells, cellular GSH is depleted, leading to increased ROS levels [34]. Notably, Tsvetkov and colleagues have explored the mechanism of copper-induced cell death, revealing that copper can induce aggregation of lipid-acylated proteins and loss of iron-sulfur (Fe-S) cluster proteins by binding directly to the lipid-acylated component of the TCA cycle, ultimately increasing ROS and causing cell death [4]. Despite treatment options such as surgical resection, chemotherapy, and targeted therapy, outcomes for advanced-stage ovarian cancer remain unsatisfactory. Exploiting the ROS susceptibility of cancer cells and the mechanism of cuproptosis may hold promise for ovarian cancer treatment.

In this study, we analyzed the differential expression and prognostic value of cuproptosis-related genes in ovarian cancer. We found that LIAS and MTF1 act as protective factors for patients with ovarian cancer in GSE140082. Cuproptosis occurs through the direct binding of copper to acylated components of the tricarboxylic acid cycle. This leads to aggregation of acylated proteins and subsequent loss of iron-sulfur cluster proteins, resulting in protein toxicity stress and ultimately cell death [4]. LIAS, associated with iron-sulfur clusters rather than directly with copper, is an enzyme located in the mitochondria that plays a critical role in the biosynthesis of lipoic acid, an essential cofactor involved in mitochondrial energy metabolism [35]. Maintaining effective mitochondrial function is crucial for providing energy to rapidly dividing cells and overcoming oxidative stress. LIAS contributes to mitochondrial health and energy production by promoting the biosynthesis of lipoic acid [36]. Adequate levels of lipoic acid and proper mitochondrial function may help cells resist metabolic stresses associated with cancer growth. MTF1 is a transcription factor that plays a crucial role in regulating the expression of genes involved in metal ion homeostasis,

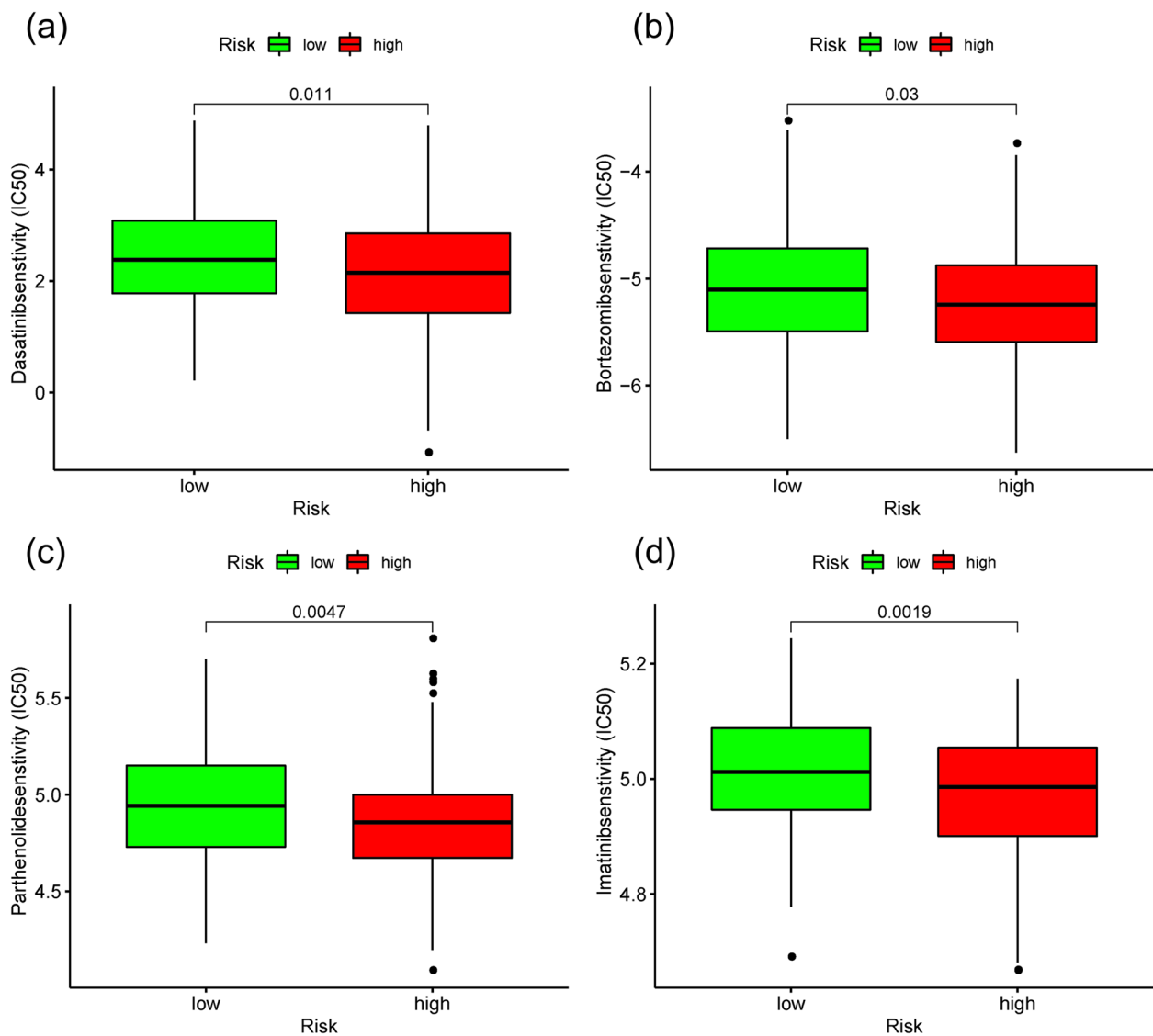


Fig. 6 Prediction of potential therapeutic agents against ovarian cancer based on risk score. **A–D** Comparison of estimated IC50 values of Dasatinib (A), Bortezomib (B), Parthenolide (C), and Imatinib (D) in high and low risk groups

particularly copper. It binds to specific DNA sequences called metal response elements to activate or repress target genes in response to changes in metal levels within cells [37]. Dysregulation of copper levels can affect oxidative stress responses and other pathways involved in cancer progression. Furthermore, the prognostic value of LIAS and MTF1 in ovarian cancer was validated using four external GEO datasets. Subsequently, a risk model incorporating MTF1 and LIAS was developed, dividing ovarian cancer patients into high- and low-risk groups. Survival analysis revealed that a higher risk score was significantly associated with poor OS. Additionally, we investigated the relationship between risk

groups and pathways related to tumor progression and metabolism. The results revealed that angiogenesis and EMT were enriched in the high-risk group. Accumulating evidence indicates that copper promotes angiogenesis by activating several angiogenic factors, including vascular endothelial growth factor, hypoxia-inducible factor-1 (HIF1), and interleukin-1 [34, 38, 39]. Regarding EMT, copper exposure can induce EMT through the activation of MAPKs and upregulation of MMP-3 [40]. Vitaliti et al. elucidated that copper plays a crucial role in AKT-driven EMT activation [41]. Furthermore, the relationship between risk groups and tumor progression, as well as metabolism-related pathways, was explored.

The results indicated enrichment of angiogenesis and EMT pathways in the high-risk group. Moreover, LIAS and MTF1 have been reported to play important roles in angiogenesis and EMT [42–44].

The association between the expression of LIAS or MTF1 and immune cells was explored using single-cell RNA sequencing. LIAS expression was predominantly detected in T cells, B cells, and macrophages, while both LIAS and MTF1 were enriched in B cells, macrophages, and endothelial cells. Additionally, using TIMER datasets, we analyzed the correlation between LIAS or MTF1 and immune cells. The results showed that LIAS was positively correlated with CD4 and CD8+ T cells, whereas MTF1 was positively correlated with macrophages. It is known that high infiltration of T cells indicates a favorable prognosis. The tumor macrophage environment often includes a significant presence of M2 macrophages, which play crucial roles in upregulating immunosuppressive proteins, promoting angiogenesis, tumor invasion, metastasis, and suppressing T cell function [45]. Immune therapies have shown limited efficacy in ovarian cancer. Wang et al. analyzed the tumor microenvironment of patients who responded to immunotherapy and found that increased efficacy of immune therapies in ovarian cancer is associated with state changes of NK cells and small subsets of CD8 T cells into active and cytotoxic states [46]. Immune checkpoint inhibitors (ICIs) are administered in clinical practice for treating ovarian cancer, and we investigated whether the risk model was related to ICI-related biomarkers. The results revealed that high-risk scores were positively correlated with high expression of CD276, PDCD1, CD44, LAG3, and CD160. Furthermore, patients in the high-risk group with a higher fraction of CD4+ naïve T cells, M2 macrophages, and follicular helper T cells in the tumor immune microenvironment had a higher TIDE score. These findings suggest that patients in the high-risk group are more likely to experience immune escape.

To explore potential molecular targets of LIAS and MTF1, Cellminer, CTRP, and GDSC were used to analyze effective drugs. The IC50 values of six drugs—LMP776, Vorinostat, Palbociclib, Dromostanolone Propionate, Nitrogen mustard, and Cladribine—were lower in the low-LIAS group. LMP776, an indenoisoquinoline topoisomerase I (TOP1) inhibitor, is currently in clinical development for ovarian cancer and addresses issues such as chemical instability, short plasma half-life, and severe diarrhea associated with camptothecin derivatives, which are FDA approved for ovarian cancer treatment [47]. There is overexpression of histone deacetylases 1–3 in patients with ovarian cancer. Vorinostat, a selective inhibitor of histone deacetylase 2, has been approved as a therapeutic strategy for ovarian cancer treatment [48].

Surprisingly, Palbociclib, a CDK4/6 inhibitor, has shown limited efficacy as a single agent due to resistance in ovarian cancer [49]. Additionally, the sensitivity of gemcitabine and vincristine was negatively correlated with the expression of MTF1 or LIAS. Vincristine, belonging to the vinca alkaloid group, is FDA approved for leukemia treatment and has several off-label uses in ovarian cancer [50]. Furthermore, we observed that the IC50 values of Dasatinib, Bortezomib, Parthenolide, and Imatinib were significantly lower in the high-risk group. Dasatinib, an SFK inhibitor, has been shown to promote overall survival benefits and inhibit peritoneal dissemination of ovarian cancer [51, 52]. Depletion of plasma cells by Bortezomib reversed mesenchymal characteristics of ovarian cancer and inhibited tumor growth in vivo [53]. However, other researchers have reported disappointing result with Bortezomib in ovarian cancer treatment and noted its potential adverse effects on ovarian function by accelerating ovarian reserve depletion, leading to fertility problems [54, 55]. Parthenolide, an Hsp90 inhibitor, induces cancer cell death through activation of caspase-8- and Bid-dependent pathways and the mitochondria-mediated apoptotic pathway [56]. Imatinib suppresses cancer cell proliferation by acting on platelet-derived growth factor receptor alpha and Akt [57]. Extensive clinical studies are needed to verify whether these drugs can effectively treat high-risk patients. Moreover, the specific mechanisms and potential side effects of these drugs must be investigated through in vitro and in vivo experiments.

Despite these noteworthy observations, there are still some limitations. Firstly, we matched each solid cancer type in TCGA with the corresponding healthy tissue in GTEx. As the source of patients and specific information is not clear, there will be some bias in this comparison. Secondly, this study mostly focused on bioinformatic analysis, and additional in vitro and in vitro and vivo experiments may be necessary to verify our results, which will be further improved in the future.

Conclusions

Generally, the study provides a comprehensive overview of cuproptosis-related genes in ovarian cancer and established a prognostic risk model for ovarian cancer patients, which is composed of LIAS and MTF1. The prognostic risk model demonstrates strong performance in predicting OS among ovarian cancer patients. Additionally, clinical characteristics, tumor progression, metabolism-related pathways, immune landscape, and drug sensitivity were analyzed across two risk groups of ovarian cancer patients, revealing significant distinctions between the groups. Specifically, patients in the high-risk group may exhibit poor response to immunotherapy but

could be sensitive to certain chemotherapeutic agents. In summary, the study highlights the potential clinical relevance of cuproptosis-related genes and offers novel insights into the development of pharmacological strategies targeting cuproptosis for the prevention and treatment of ovarian cancer.

Abbreviations

MTF1	Metal Regulatory Transcription Factor 1
LIAS	Lipoic Acid Synthetase
TCA	Tricarboxylic acid
CNV	Copy Number Variation
LASSO	The least absolute shrinkage and selection operator
TCGA	The Cancer Genome Atlas
GTE _x	Genotype-Tissue Expression
GEO	Gene Expression Omnibus
KM	Kaplan–Meier
HR	Hazard ratio
CI	Confidence interval
OS	Overall survival
ROC	Receiver operating characteristic
AUC	Area under the curve
PPI	Protein-protein interactions
GO	Gene Ontology
KEGG	Kyoto Encyclopedia of Genes and Genomes
EMT	Epithelial-mesenchymal transition
TISCH	Tumor Immune Single-Cell Hub
TIDE	Tumor Immune Dysfunction and Exclusion
FDA	Food and Drug Administration
CTRP	Cancer Therapeutics Response Portal
GDSC	Genomics of Drug Sensitivity in Cancer
ICI	Immune checkpoint inhibitor
ROS	Reactive oxygen species
TOP1	Topoisomerase I

Supplementary Information

The online version contains supplementary material available at <https://doi.org/10.1186/s12905-024-03519-9>.

Supplementary Material 1.
Supplementary Material 2.
Supplementary Material 3.
Supplementary Material 4.
Supplementary Material 5.
Supplementary Material 6.
Supplementary Material 7.
Supplementary Material 8.
Supplementary Material 9.

Acknowledgements

We sincerely thank the data provided by TCGA and GEO databases, the equipment and experimental guidance of Renmin Hospital Central Laboratory, and thank all the staff of obstetrics and gynecology for their support during the study.

Authors' contributions

WT and FF-D wrote the main manuscript text. QY-C prepared Figs. 1 and 2. ZM-D improved the writing style and addressed grammatical errors. HL prepared Figs. 3, 4, 5 and 6. YX-C guided the research idea of the full text. All authors reviewed the manuscript and approved the final manuscript.

Funding

This work was supported by cross-innovation talent project in Renmin Hospital of Wuhan University (grant number JCRCZN-2022-016); Natural Science Foundation of Hubei Province (grant number 2022CFB252); Undergraduate education quality construction comprehensive reform project (grant number 2022ZG282) and the National Natural Science Foundation of China (grant number 82071655).

Data availability

The datasets generated and analyzed during the current study are available in TCGA (<https://portal.gdc.cancer.gov/>), GTEx (<http://commonfund.nih.gov/GTEx/data>) and GEO (<https://www.ncbi.nlm.nih.gov/geo/>) databases.

Declarations

Ethics approval and consent to participate

Not applicable.

Consent for publication

Not applicable.

Competing interests

The authors declare no competing interests.

Received: 27 January 2024 Accepted: 17 December 2024

Published online: 24 January 2025

References

- Sung H, Ferlay J, Siegel RL, et al. Global Cancer Statistics. 2020: GLOBOCAN estimates of incidence and mortality worldwide for 36 cancers in 185 Countries. *CA Cancer J Clin.* 2021;71(3):209–49. <https://doi.org/10.3322/caac.21660>.
- Stewart C, Ralyea C, Lockwood S. Ovarian Cancer: an Integrated Review. *Semin Oncol Nurs.* 2019;35(2):151–6. <https://doi.org/10.1016/j.soncn.2019.02.001>.
- Lheureux S, Braunstein M, Oza AM. Epithelial ovarian cancer: evolution of management in the era of precision medicine. *CA Cancer J Clin.* 2019;69(4):280–304. <https://doi.org/10.3322/caac.21559>.
- Tsvetkov P, Coy S, Petrova B, et al. Copper induces cell death by targeting lipoylated TCA cycle proteins. *Science.* 2022;375(6586):1254–61. <https://doi.org/10.1126/science.abf0529>.
- Saleh SAK, Adly HM, Abdelkhalik AA, et al. Serum levels of Selenium, Zinc, Copper, Manganese, and Iron in prostate Cancer patients. *Curr Urol.* 2020;14(1):44–9. <https://doi.org/10.1159/000499261>.
- Jin Y, Zhang C, Xu H, et al. Combined effects of serum trace metals and polymorphisms of CYP1A1 or GSTM1 on non-small cell lung cancer: a hospital based case-control study in China. *Cancer Epidemiol.* 2011;35(2):182–7. <https://doi.org/10.1016/j.canep.2010.06.004>.
- Pavithra V, Sathisha TG, Kasturi K, et al. Serum levels of metal ions in female patients with breast cancer. *J Clin Diagn Res.* 2015;9(1):BC25–c27. <https://doi.org/10.7860/JCDR/2015/11627.5476>.
- Caglayan A, Katlan DC, Tuncer ZS, et al. Evaluation of trace elements associated with antioxidant enzymes in blood of primary epithelial ovarian cancer patients. *J Trace Elem Med Biol.* 2019;52:254–62. <https://doi.org/10.1016/j.jtemb.2019.01.010>.
- Zheng P, Zhou C, Lu L, et al. Elesclomol: a copper ionophore targeting mitochondrial metabolism for cancer therapy. *J Exp Clin Cancer Res.* 2022;41(1):271. <https://doi.org/10.1186/s13046-022-02485-0>.
- Lu X, Chen X, Lin C, et al. Elesclomol Loaded Copper Oxide Nanoparticle triggers cuproptosis to Enhance Antitumor Immunotherapy. *Adv Sci (Weinh).* 2024;11(18):e2309984. <https://doi.org/10.1002/adv.202309984>.
- Guo B, Yang F, Zhang L, et al. Cuproptosis Induced by ROS responsive nanoparticles with Elesclomol and Copper Combined with alphaPD-L1 for enhanced Cancer Immunotherapy. *Adv Mater.* 2023;35(22):e2212267. <https://doi.org/10.1002/adma.202212267>.

12. Lin S, Yang H. Ovarian cancer risk according to circulating zinc and copper concentrations: a meta-analysis and mendelian randomization study. *Clin Nutr*. 2021;40(4):2464–8. <https://doi.org/10.1016/j.clnu.2020.10.011>.
13. Mohammed Asiri S, Levina A, New EJ, et al. Investigations of cellular copper metabolism in ovarian cancer cells using a ratiometric fluorescent copper dye. *J Biol Inorg Chem*. 2022. <https://doi.org/10.1007/s00775-022-01978-9>.
14. Arnesano F, Natile G. Interference between copper transport systems and platinum drugs. *Semin Cancer Biol*. 2021;76:173–88. <https://doi.org/10.1016/j.semcancer.2021.05.023>.
15. Lukanovic D, Herzog M, Kobal B, et al. The contribution of copper efflux transporters ATP7A and ATP7B to chemoresistance and personalized medicine in ovarian cancer. *Biomed Pharmacother*. 2020;129:110401. <https://doi.org/10.1016/j.biopha.2020.110401>.
16. Tong X, Tang R, Xiao M, et al. Targeting cell death pathways for cancer therapy: recent developments in necroptosis, pyroptosis, ferroptosis, and cuproptosis research. *J Hematol Oncol*. 2022;15(1):174. <https://doi.org/10.1186/s13045-022-01392-3>.
17. Zhan S, Yung MMH, Siu MKY, et al. New insights into Ferroptosis Initiating therapies (FIT) by targeting the rewired lipid metabolism in Ovarian Cancer Peritoneal metastases. *Int J Mol Sci*. 2022;23(23). <https://doi.org/10.3390/ijms232315263>.
18. Zhang C, Liu N. Ferroptosis, necroptosis, and pyroptosis in the occurrence and development of ovarian cancer. *Front Immunol*. 2022;13:920059. <https://doi.org/10.3389/fimmu.2022.920059>.
19. Xie J, Yang Y, Gao Y, et al. Cuproptosis: mechanisms and links with cancers. *Mol Cancer*. 2023;22(1):46. <https://doi.org/10.1186/s12943-023-01732-y>.
20. Consortium GT. The genotype-tissue expression (GTEx) project. *Nat Genet*. 2013;45(6):580–5. <https://doi.org/10.1038/ng.2653>.
21. Lanczky A, Györfy B. Web-based Survival Analysis Tool tailored for Medical Research (KMplot): development and implementation. *J Med Internet Res*. 2021;23(7):e27633. <https://doi.org/10.2196/27633>.
22. Tan W, Liu S, Deng Z, et al. Gene signature of m6A-related targets to predict prognosis and immunotherapy response in ovarian cancer. *J Cancer Res Clin Oncol*. 2022. <https://doi.org/10.1007/s00432-022-04162-3>.
23. Szklarczyk D, Franceschini A, Wyder S, et al. STRING v10: protein-protein interaction networks, integrated over the tree of life. *Nucleic Acids Res*. 2015;43(Database issue):D447–452. <https://doi.org/10.1093/nar/gku1003>.
24. Peng X, Chen Z, Farshidfar F, et al. Molecular characterization and clinical relevance of metabolic expression subtypes in human cancers. *Cell Rep*. 2018;23(1):255–e269254. <https://doi.org/10.1016/j.celrep.2018.03.077>.
25. Newman AM, Liu CL, Green MR, et al. Robust enumeration of cell subsets from tissue expression profiles. *Nat Methods*. 2015;12(5):453–7. <https://doi.org/10.1038/nmeth.3337>.
26. Sun D, Wang J, Han Y, et al. TISCH: a comprehensive web resource enabling interactive single-cell transcriptome visualization of tumor microenvironment. *Nucleic Acids Res*. 2021;49(D1):D1420–30. <https://doi.org/10.1093/nar/gkaa1020>.
27. Fu J, Li K, Zhang W, et al. Large-scale public data reuse to model immunotherapy response and resistance. *Genome Med*. 2020;12(1):21. <https://doi.org/10.1186/s13073-020-0721-z>.
28. Ghandi M, Huang FW, Jane-Valbuena J, et al. Next-generation characterization of the Cancer Cell Line Encyclopedia. *Nature*. 2019;569(7757):503–8. <https://doi.org/10.1038/s41586-019-1186-3>.
29. Giannini A, Di Dio C, Di Donato V, et al. PARP inhibitors in newly diagnosed and recurrent ovarian cancer. *Am J Clin Oncol*. 2023;46(9):414–9. <https://doi.org/10.1097/JCO.0000000000001024>.
30. Perrone C, Angioli R, Luvero D, et al. Targeting BRAF pathway in low-grade serous ovarian cancer. *J Gynecol Oncol*. 2024. <https://doi.org/10.3802/jgo.2024.35.e104>.
31. Aubert L, Nandagopal N, Steinhart Z, et al. Copper bioavailability is a KRAS-specific vulnerability in colorectal cancer. *Nat Commun*. 2020;11(1):3701. <https://doi.org/10.1038/s41467-020-17549-y>.
32. Baltaci AK, Dundar TK, Aksoy F, et al. Changes in the serum levels of Trace Elements before and after the operation in thyroid Cancer patients. *Biol Trace Elem Res*. 2017;175(1):57–64. <https://doi.org/10.1007/s12011-016-0768-2>.
33. Chen F, Wang J, Chen J, et al. Serum copper and zinc levels and the risk of oral cancer: a new insight based on large-scale case-control study. *Oral Dis*. 2019;25(1):80–6. <https://doi.org/10.1111/odi.12957>.
34. Oliveri V. Selective targeting of Cancer cells by copper ionophores: an overview. *Front Mol Biosci*. 2022;9:841814. <https://doi.org/10.3389/fmolb.2022.841814>.
35. Krishnamoorthy E, Hassan S, Hanna LE, et al. Homology modeling of Homo sapiens lipoic acid synthase: substrate docking and insights on its binding mode. *J Theor Biol*. 2017;420:259–66. <https://doi.org/10.1016/j.jtbi.2016.09.005>.
36. Hendricks AL, Wachnowsky C, Fries B, et al. Characterization and reconstitution of human lipoyl synthase (LIAS) supports ISCA2 and ISCU as primary cluster donors and an ordered mechanism of Cluster Assembly. *Int J Mol Sci*. 2021;22(4). <https://doi.org/10.3390/ijms22041598>.
37. Zhao J, Guo S, Schrodi SJ, et al. Cuproptosis and cuproptosis-related genes in rheumatoid arthritis: implication, prospects, and perspectives. *Front Immunol*. 2022;13:930278. <https://doi.org/10.3389/fimmu.2022.930278>.
38. Ge EJ, Bush AI, Casini A, et al. Connecting copper and cancer: from transition metal signalling to metalloplasia. *Nat Rev Cancer*. 2022;22(2):102–13. <https://doi.org/10.1038/s41568-021-00417-2>.
39. Lelievre P, Sancey L, Coll JL, et al. The multifaceted roles of copper in Cancer: a Trace Metal element with Dysregulated Metabolism, but also a Target or a bullet for Therapy. *Cancers (Basel)*. 2020;12(12). <https://doi.org/10.3390/cancers12123594>.
40. Zhang Y, Mo Y, Yuan J, et al. MMP-3 activation is involved in copper oxide nanoparticle-induced epithelial-mesenchymal transition in human lung epithelial cells. *Nanotoxicology*. 2021;15(10):1380–402. <https://doi.org/10.1080/17435390.2022.2030822>.
41. Vitaliti A, Roccatani I, Iorio E, et al. AKT-driven epithelial-mesenchymal transition is affected by copper bioavailability in HER2 negative breast cancer cells via a LOXL2-independent mechanism. *Cell Oncol (Dordr)*. 2022. <https://doi.org/10.1007/s13402-022-00738-w>.
42. Burr SP, Costa AS, Grice GL, et al. Mitochondrial protein lipoylation and the 2-Oxoglutarate dehydrogenase Complex Controls HIF1α Stability in Aerobic conditions. *Cell Metab*. 2016;24(5):740–52. <https://doi.org/10.1016/j.cmet.2016.09.015>.
43. Ji L, Zhao G, Zhang P, et al. Knockout of MTF1 inhibits the epithelial to mesenchymal transition in Ovarian Cancer cells. *J Cancer*. 2018;9(24):4578–85. <https://doi.org/10.7150/jca.28040>.
44. Zhang R, Zhao G, Shi H, et al. Zinc regulates primary ovarian tumor growth and metastasis through the epithelial to mesenchymal transition. *Free Radic Biol Med*. 2020;160:775–83. <https://doi.org/10.1016/j.freeradbiomed.2020.09.010>.
45. Anderson NR, Minutolo NG, Gill S, et al. Macrophage-based approaches for Cancer Immunotherapy. *Cancer Res*. 2021;81(5):1201–8. <https://doi.org/10.1158/0008-5472.CAN-20-2990>.
46. Wan C, Keany MP, Dong H, et al. Enhanced efficacy of simultaneous PD-1 and PD-L1 Immune Checkpoint Blockade in High-Grade Serous Ovarian Cancer. *Cancer Res*. 2021;81(1):158–73. <https://doi.org/10.1158/0008-5472.CAN-20-1674>.
47. Marzi L, Szabova L, Gordon M, et al. The Indenoisoquinoline TOP1 inhibitors selectively target homologous recombination-deficient and Schlafen 11-Positive Cancer cells and synergize with Olaparib. *Clin Cancer Res*. 2019;25(20):6206–16. <https://doi.org/10.1158/1078-0432.CCR-19-0419>.
48. Shetty MG, Pai P, Deaver RE, et al. Histone deacetylase 2 selective inhibitors: a versatile therapeutic strategy as next generation drug target in cancer therapy. *Pharmacol Res*. 2021;170:105695. <https://doi.org/10.1016/j.phrs.2021.105695>.
49. Liu C, Huang Y, Qin T, et al. AZD5153 reverses palbociclib resistance in ovarian cancer by inhibiting cell cycle-related proteins and the MAPK/PI3K-AKT pathway. *Cancer Lett*. 2022;528:31–44. <https://doi.org/10.1016/j.canlet.2021.12.021>.
50. Below J. J MD. Vincristine. StatPearls: Treasure Island (FL); 2022.
51. Kawata M, Kondo J, Onuma K, et al. Polarity switching of ovarian cancer cell clusters via SRC family kinase is involved in the peritoneal dissemination. *Cancer Sci*. 2022;113(10):3437–48. <https://doi.org/10.1111/cas.15493>.
52. Lui GYL, Shaw R, Schaub FX, et al. BET, SRC, and BCL2 family inhibitors are synergistic drug combinations with PARP inhibitors in ovarian cancer. *EBioMedicine*. 2020;60:102988. <https://doi.org/10.1016/j.ebiom.2020.102988>.

53. Yang Z, Wang W, Zhao L, et al. Plasma cells shape the mesenchymal identity of ovarian cancers through transfer of exosome-derived microRNAs. *Sci Adv.* 2021;7(9). <https://doi.org/10.1126/sciadv.abb0737>.
54. Anchoori RK, George L, Tseng SH, et al. Chirality and asymmetry increase the potency of candidate ADRM1/RPN13 inhibitors. *PLoS ONE.* 2021;16(9):e0256937. <https://doi.org/10.1371/journal.pone.0256937>.
55. Mutluay D, Tenekeci GY, Monsef YA. Bortezomib-Induced ovarian toxicity in mice. *Toxicol Pathol.* 2022;50(3):381–9. <https://doi.org/10.1177/01926233221083527>.
56. Lee CS, Kim YJ, Lee SA, et al. Combined effect of Hsp90 inhibitor geldanamycin and parthenolide via reactive oxygen species-mediated apoptotic process on epithelial ovarian cancer cells. *Basic Clin Pharmacol Toxicol.* 2012;111(3):173–81. <https://doi.org/10.1111/j.1742-7843.2012.00883.x>.
57. Matei D, Chang DD, Jeng MH. Imatinib mesylate (gleevec) inhibits ovarian cancer cell growth through a mechanism dependent on platelet-derived growth factor receptor alpha and akt inactivation. *Clin Cancer Res.* 2004;10(2):681–90. <https://doi.org/10.1158/1078-0432.ccr-0754-03>.

Publisher's note

Springer Nature remains neutral with regard to jurisdictional claims in published maps and institutional affiliations.